International Journal of Recent Technology and Engineering (IJRTE)
ISSN: 2277-3878 (Online), Volume-8 Issue-6, March 2020

Moment Redistribution in Continuous RC Beams Top Strengthened with Steel and CFRP Plates

Amr Ibrahim, Ayman Khalil, Shady Salem, Mahmoud El-Kateb

Abstract*: *It is common practice to retrofit continuous reinforced concrete (RC) beams by fiber reinforced polymer (FRP) or steel plates. This can cause a significant amount of moment redistribution (MR) which results in an efficient and economic design when taken into consideration. There is lack in research regarding MR in continuous RC beams when strengthening plates are applied only at the top side at the hogging regions. The main purpose of this paper is to assess MR in continuous RC beams top strengthened with steel and/or carbon fiber reinforced polymer (CFRP) plates. In this respect, a nonlinear finite element model was developed using ABAQUS 6.14 and validated using experimental research program. The model was found capable of stimulating the behavior of such beams and hence assessing the percentage of MR which can be achieved using steel and CFRP strengthening. A parametric study is conducted to investigate the effect of various parameters, different from those investigated in the experimental program, on the MR in continuous RC beams. Parameters related to the concrete compressive strength, reinforcement ratio, beam thickness and thickness of strengthening plates were considered in this study. The results showed that significant amounts of MR can be achieved using either steel or CFRP plates and that MR is enhanced with the change in concrete compressive strength. Moreover, it was found out that the change in steel bars reinforcement ratio or in thickness of the strengthening plates has different effect on the beams strengthened with steel plates than those strengthened with CFRP plates.

Keywords* : *Moment redistribution, strengthening, steel plates, CFRP plates

I. INTRODUCTION

There are various reasons to which existing continuous reinforced concrete (RC) beams may need strengthening or retrofitting, increasing the flexural strength, ductility or even durability. Strengthening using steel plates has many advantages regarding increasing the strength and ductility of the beams, as well as the adequate bond strength with concrete. Moreover, adding fiber-reinforced polymer (FRP) materials to RC structures was found to be an effective technique to improve the strength and durability of such structures [1,2]. However, research has revealed that FRP strengthening of flexural members reduces the ductility prior to FRP debonding [3-6]. The elastic nature of the FRP generally leads to a more brittle failure of FRP-strengthened RC members. Strengthening of Continuous RC beams often leads to significant amounts of moment redistribution (MR) which is usually carried out by increasing the moments at the sagging zones and reducing the moments over supports [7]. This is done by the application of the strengthening plates at the sagging regions of the beams between the supports, or at both the sagging and hogging zones [4].

The previous research on externally bonded (EB) and near surface mounted (NSM) plated structures was mainly addressing the bond behavior between the plate and the concrete interface [8-10]. Researchers have also developed different approaches to measure the ductility of beams when having external strengthening [4,11], but none of them is used to quantify the MR of continuous plated structures. Furthermore, the design guidelines [12,13] tend to neglect the effect of MR in plated structures. However, previous carried out tests clearly show that significant amounts of MR can be obtained in both EB and NSM plated beams [14-16]. These tests were carried out on beams strengthened at the sagging zones between supports only or at both the sagging and hogging regions. However, there is a lack in research regarding MR in continuous RC beams only top strengthened at the hogging zones.

This paper presents a numerical investigation for the MR in continuous RC beams when top strengthening plates are applied to the hogging zones of those beams. This is to deeply assess the strength and flexural behavior of top plated RC beams. The numerical study includes the development of finite element (FE) models, capable of simulating the non-linear behavior of reinforced concrete. The models were first calibrated and validated with the results of an experimental program, which was conducted on a set of eight top strengthened continuous beams. Then, the validated models were used to simulate the response of full-scale continuous two span concrete beams top strengthened with steel and CFRP plates. A parametric study is performed to investigate the effect of different factors than those studied in the experimental analysis.

Manuscript received on February 10, 2020.
Revised Manuscript received on February 20, 2020.
Manuscript published on March 30, 2020.
* Correspondence Author
Amr Ibrahim*, The British University, Egypt/Civil Engineering Department, Cairo, Egypt. Email: amr.ibrahim@bue.edu.eg
Shady Salem, The British University, Egypt/Civil Engineering Department, Cairo, Egypt. Email: shady.salem@bue.edu.eg
Ayman Khalil, Structural Engineering Department, Ain Shams University, Cairo, Egypt. Email: ayman.khalil@eng.asu.edu.eg
Mahmoud El-Kateb, Structural Engineering Department, Ain Shams University, Cairo, Egypt. Email: mahmoud.elkateb@eng.asu.edu.eg

This would help structural engineers to predict the amount of MR, ultimate load carrying capacity and deflection values in top plated beams.

II. EXPERIMENTAL PROGRAM

The beams, which were tested in the experimental program, had two spans with span length of two meters. The beams were loaded by two concentrated loads, each load was applied at the mid-span. Figure 1 shows the configuration of the test specimens, location of the loads and position of installed strengthening plates. The cross sections of the beams were designed as T-sections to increase the flexural capacity of the section at mid-span between the supports and to avoid early failure of the beam at mid-span section, this will permit higher amounts of MR to occur at the ultimate load capacity of the tested specimens. The beams had a width of 200 mm and height of 350mm. The used plates were implemented at the flanges of the beam within the effective width of the slab rather than in the web of the beam to avoid the presence of an intermediate column if any. The dimensions of the steel plates were 50 mm in width and 6 mm in thickness, while the CFRP laminates were of 50 mm in width and 1.2 mm in thickness. The length of all strengthening plates was 1500 mm.

Table 1 summarizes the test matrix showing the tested parameters. The labelling scheme for strengthened beams depend on the type, number and method of installment of the used plates. These symbols start with a letter C or S depending on the material of the plate, C for carbon and S for Steel, followed by a letter E or N depending on the method of installment of the plate where E is for externally bonded and N is for Near surface mounted, followed by a digit indicating the number of used plates. For example, beam CN1 is strengthened with 1 NSM CFRP plate, while beam SE1 is strengthened with 1 steel externally bonded plate.

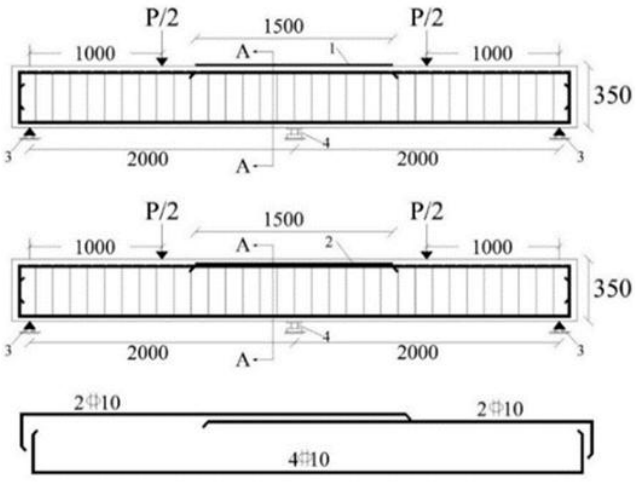

Fig. 1.Test setup (dimensions in mm). 1 - Steel or CFRP EB plate; 2 - Steel or CFRP NSM plate; 3 - roller support, 4 - load cell.

III. TEST RESULTS

For the tested beams, a linear elastic analysis was considered to predict their failure loads, and the corresponding moments at the sagging and hogging zones. Table 2 lists the predicted and the experimental bending moments at the central support and at the mid-span cross-sections of all the beams. M_{sag}.and $M_{hog.}$ are the experimental sagging and hogging moments, while $M_{sag.el}$ and $M_{hog.el}$ are the flexural moments in the sagging and hogging zones at the elastic state without any form of moment redistribution and were calculated by eqs. (1) & (2) which were used in the study done by Aiello et al. [17]. The stiffness of the beams was conventionally considered to be constant along the whole length. The percentages of change, M_{sag} & M_{hog} were calculated using eqs (3) & (4). The average percentage of MR was calculated by taking the mean value of both $M_{sag.el}$ and $M_{hog.el}$, but after changing the sign of $M_{sag.el}$. The symbol l refers to the span length, while a is the distance of applied loads (0.5Pu) from the central and end supports respectively.

$$M_{sag.el} = \frac{(2l^3 - 3al^2 + a^3)}{4l^3} aP_u \quad (1)$$

$$M_{hog.el} = -\frac{a(l^2 - a^2)}{4l^2} P_u \quad (2)$$

$$[\%]\ of\ change, M_{sag} = \left(\frac{M_{sag} - M_{sag.el}}{M_{sag.el}}\right) * 100 \quad (3)$$

$$[\%]\ of\ change,\ M_{hog} = \left(\frac{M_{hog} - M_{hog.el}}{M_{hog.el}}\right) * 100 \quad (4)$$

Table 1. Test matrix

Specimen	Material of plate	Number of plates	Method of Installment
B1	No plates (Control)	---	---
SN1	Steel	1	NSM
SE1	Steel	1	EB
SN2	Steel	2	NSM
SE2	Steel	2	EB
CN1	CFRP	1	NSM
CE1	CFRP	1	EB
CN2	CFRP	2	NSM

It was noticed in table 2, that the control beam recorded a significant amount of average MR without strengthening. All the beams have seen moment redistributions from the sagging to the hogging zones, Beams SN2 and SE2 had the highest average values of MR with 70.69 % and 64.67 % respectively. Beam CE1 had a sufficient amount of MR with 39.52 % which is higher than that recorded by beam B1 despite the debonding that occurred between the CFRP plate and the concrete surface.

IV. NUMERICAL MODELING

Eight specimens were modelled using ABAQUS 6.14 [18] to simulate the behavior of top strengthened RC continuous beams. This was carried out to verify the FE models against the experimental results in terms of load-deflection, and load strain responses. The accuracy of the results mainly relies on the FE mesh, constitutive material models and the boundary conditions. Therefore, these aspects are accurately investigated in the proposed FE model.

In the current model. The mesh intensity is kept the same for the whole concrete part of the model, as shown in Fig. 2.

Table 2. Test results

Specimen	P_u	$M_{sag.}$	$M_{hog.}$	$M_{sag.el}$	$M_{hog.el}$	[%] of change, M_{sag}	[%] of change, M_{hog}	Average [%] of MR
	kN	kN.m						
B1	467.19	53.40	-126.81	73.00	-87.60	-26.85	44.76	35.81
SN1	480.86	44.67	-151.10	75.13	-90.16	-40.55	67.59	54.07
SE1	475.00	43.88	-149.75	74.22	-89.06	-40.88	68.14	54.51
SN2	561.37	41.21	-198.27	87.71	-105.26	-53.02	88.36	70.69
SE2	525.72	42.30	-178.26	82.14	-98.57	-48.50	80.84	64.67
CN1	462.27	46.22	-138.71	72.23	-86.68	-36.02	60.03	48.02
CE1	404.71	44.50	-113.37	63.24	-75.88	-29.64	49.39	39.52
CN2	468.55	44.07	-146.14	73.21	-87.85	-39.80	66.34	53.07

A regular structured hexahedral mesh is used with a mesh size of 50 mm, as shown in Figure 2. Discrete reinforcement bars and shear stirrups were defined using three-dimensional truss elements in linear order, while the strengthening plates were defined as solid homogeneous part.

A. Steel modeling

Bi-linear model is used for steel reinforcement bars and steel plates. The Young's modulus and Poisson's ratio were taken equal to 200 GPa and 0.2 respectively. The yield and ultimate strengths for the steel reinforcement were taken equal to 360 MPa and 520 MPa, respectively. While, the same strengths were taken as 425 MPa and 566 MPa for the steel plates respectively.

B. Concrete modeling

Concrete damage plasticity model is used to model the concrete. The compressive strength defined in this study is 28.7 MPa. The values of stress and inelastic strain in both the compressive behavior and compression damage were evaluated with respect to the concrete characteristic compressive strength and the modulus of elasticity. Also, the values of stress and cracking strain in both the tensile behavior and tension damage were also determined according to the concrete compressive strength and modulus of elasticity. Tension stiffening is used to model the post-failure behavior for direct tension across cracks, which allows the definition of the strain softening behavior for cracked concrete. The total strain at which the tensile stress is reduced to 10% of its maximum value is taken in previous studies as 8.7 times the tensile cracking strain as shown in figure 3.

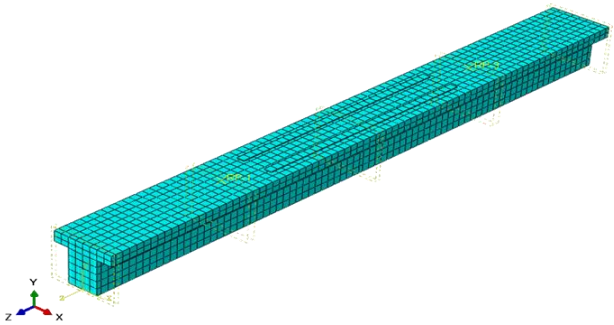

Fig. 2.Typical finite element mesh of strengthened beams

C. Steel-concrete interaction

The interaction between the internal steel reinforcement bars and the concrete was defined using the truss in solid technique option that used in ABAQUS 6.14. This technique defines the embedded elements as truss elements simulating the reinforcement bars while the host region was specified as the continuum solid elements simulating the concrete beam. The surface-to-surface contact algorithm was used to model the contact surface between the top side of the beams and the strengthening steel plates.

D. Concrete-CFRP contact

The surface-to-surface contact between the CFRP plates and the top side of concrete was defined as cohesive behavior with damage initiation at 4 MPa in normal stresses and 6 MPa in shear stresses to stimulate the debonding of the CFRP laminate from the concrete, the damage evolution displacement type and with linear softening. The ratio of the total displacement to the plastic displacement was considered 0.1, the damage stabilization had a viscosity coefficient of 1E-5.

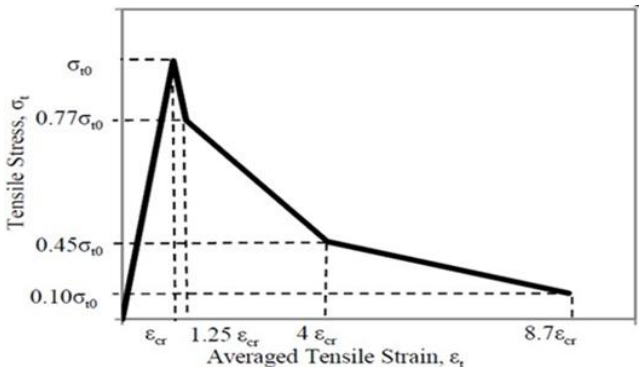

Fig. 3.Modified concrete tension stiffening model

V. MODEL VALIDATION

The finite element model is validated against the specimens tested in the experimental program. The predicted ultimate load and failure mode for each specimen were carefully examined against the test results.

The FE results, including the relations between the load and mid-span deflection and typical modes of failure for each of the models, are presented. In order to verify the FEM, a comparison between the results of the experimental tests and the finite element analysis was carried out in the following sections.

A. Strength of beams

Table 3 shows the ultimate load carrying capacity and the displacements obtained from the experimental investigation and the corresponding FEM predictions for the beams, as well as the ratio between FE and the experimental results for the ultimate loads. The table also shows the elastic stiffness values which were calculated using the loads and the displacements measured at the end of the elastic stage. The ultimate loads obtained from the finite element analysis represent the load levels at which the model failed to reach convergence which means either the concrete or the steel strain reached its ultimate value. The average ratio between the FE and experimental results for ultimate loads is 110.56% with a standard deviation of 8.82%. The Table shows that the maximum difference between the FE and experimental ultimate load was reported for beam CE1. This is due to to the debonding between the CFRP laminate and the concrete surface.

B. Deflection

Figure 4 shows the load deflection behavior regarding the experimental and FE results for all beams. According to load-deflection curves, it is noted that there is strong agreement with the experimental and FE results, especially in the elastic stage. After that, the FE load values in beams SN1, SE1, SN2, SE2 and CE1 begin to slightly increase than the experimental load values. For beam B1, it was noticed that the load deflection behavior was almost identical in the elastic stage before the experimental load values begin to decrease than the FE results until failure. For beams CN1 and CN2 the experimental and FE deflection values were almost the same throughout the whole loading process. The FE model is also considered reliable in predicting the deflection values until failure. Table 1 lists the maximum deflection values for all beams as well as the ratio between the FE and experimental results. The results show that the maximum deviation for the ultimate deflection is in the range of 10% with a standard deviation of 7.24%. The average ratio between the FE and experimental results for ultimate deflection is 104%. Regarding the elastic stiffness values for both the tested beams and FE models, it can be noted that the average ratio between the experimental and FE is in the range 107%. The maximum deviation is in the range of 12% with a standard deviation of 6.58%. These deviation values can prove the reliability of the adopted FEM results.

Beam	Failure load at each span $0.5P_u$ (kN)		Elastic Stiffness $(0.5P/\Delta)_{el.}$ (kN/mm)		Maximum Deflection (Δ_u) (mm)		% (FE / Exp.)		
	FE	Exp.	FE	Exp.	FE	Exp.	$0.5P_u$	$(0.5P/\Delta)_{el.}$	Δ_u
B1	225	234	40.63	35.87	29.78	27.15	96.42	113.27	109.69
SN1	285	240	34.47	32.12	19.98	19.36	118.65	107.31	103.20
SE1	274	238	48.55	39.15	17.51	17.13	115.49	110.70	102.22
SN2	299	281	36.9	32.98	22.02	19.61	106.55	111.89	112.29
SE2	300	263	37.95	41.41	19.62	18.63	114.19	91.64	105.31
CN1	238	231	36.43	34.68	15.99	15.93	103.14	105.04	100.38
CE1	253	202	40.81	38.53	26.22	29.75	125.23	105.90	88.13
CN2	246	234	41.29	36.75	16.02	14.44	104.80	112.35	110.94
					Average		110.56	107.26	104.02
					Standard deviation		8.82	6.58	7.24

C. Failure modes

All FEM experienced the same failure mode as the experimental specimens. Moreover, the FEM followed the same failure sequence as the experimented beams, where the failure of beams B1, SN1, SE1, CN1 and CN2 commenced through yielding of the lower steel reinforcement bars at the sagging regions. The FE results showed the failure in Beams SN2 and SE2 started with both the yielding of lower steel reinforcement at the sections near the load application points, and with the crushing of concrete at the bottom side of the concrete near the intermediate support section, which is consistent with the failure modes observed in the experimental investigation as shown in figure 5.

Furthermore, the FE model showed that instability damage for beam CE1 which resulted from the debonding of the CFRP laminate from the concrete surface which is also consistent with the experimental results. Hence, revealing is applicable for detecting the failure modes in the investigated beams whether in the tension side or in the compression side or through instability. Figure 5 shows the failure modes by the FEM for all beams and their counterpart experimental failure modes.

D. Model validation

The FE models show very good agreement with the experimental results according to the presented validation results. Due to using the simplified bi-linear modeling for the steel material, a slight difference may be observed in the plastic range between the FE models and the experimental results. Therefore, the FE models can be confidently used to extend the experimental program and investigate a wider range of parameters to investigate the effect of various factors on the flexural behavior of continuous RC beams.

VI. PARAMETRIC STUDY

A parametric study was conducted on a total of 18 beams to investigate the effect of different parameters on the MR in top plated beams. The main parameters tested in this study are the concrete compressive strength (f_{cu}), reinforcement ratio (μ), beam thickness (t_b) and the thickness of the strengthening

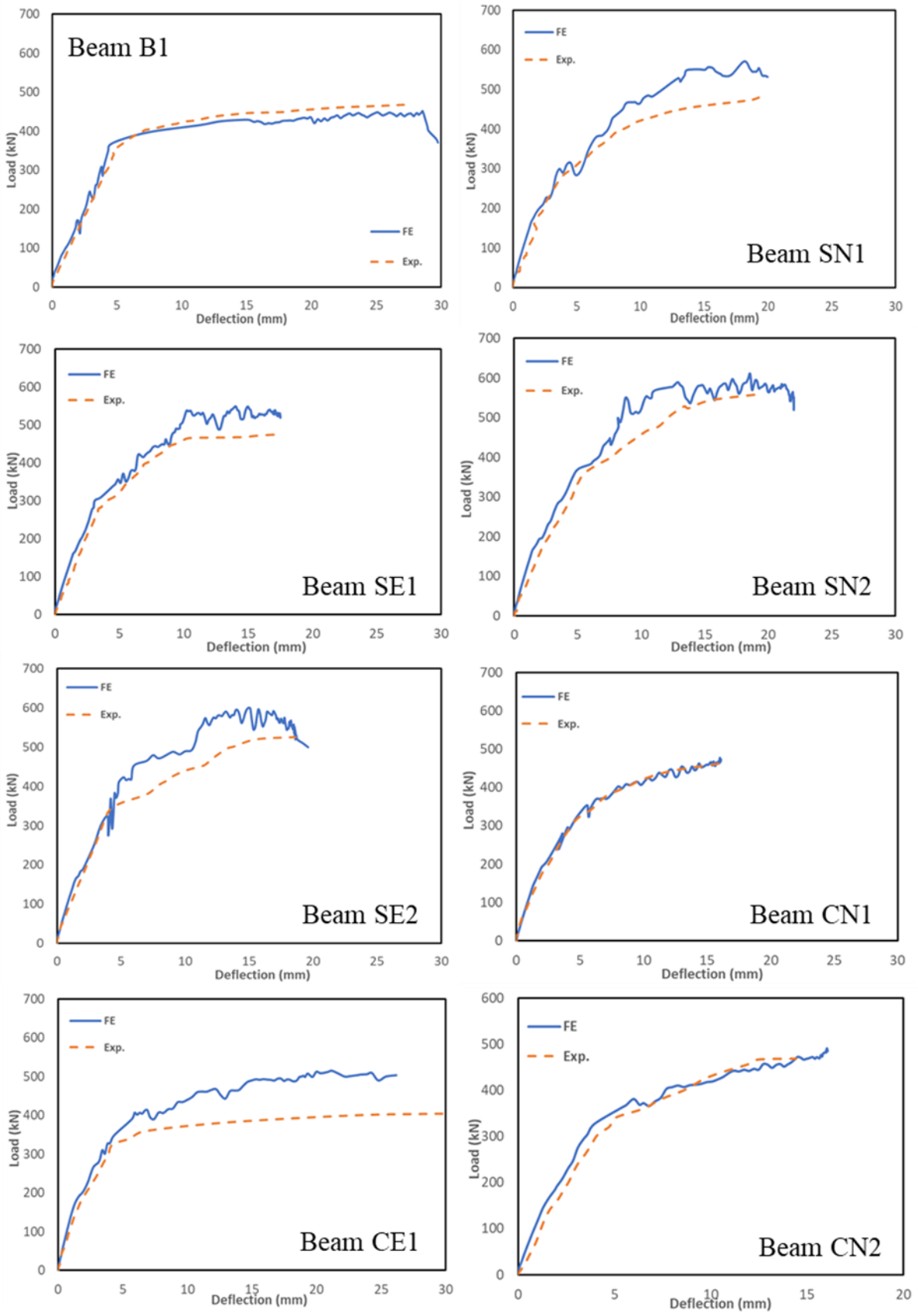

Fig. 4.Finite element results vs Experimental results

plates (t_{pl}) as shown in table 4. The NSM steel strengthening technique was applied to all the beams investigated because it was noticed in the experimental program that the steel NSM plates produced better results regarding the percentage of MR achieved and the increase in load carrying capacity than the steel EB ones, especially when 2 plates were applied. B1' to B9 were strengthened with 2 NSM steel plates, while beams B10 to B18 were strengthened with 2 NSM CFRP laminates.

Another reason for the implementation of The NSM plating technique in this study was to avoid the debonding of the CFRP plates from the upper concrete surface in beams B10 to B18.

Table 4. Details of beams in the parametric study

Beam ID		Concrete compressive strength (f_{cu}) (MPa)	Main upper and lower rft. (rft. Ratio (μ))	Beam thickness (t_b) (mm)	Thickness of plate (t_{pl}) (mm)	
Strengthened with steel plates	Strengthened with CFRP plates				Steel plates	CFRP plates
B1’	B10	25	4ϕ10 (0.47%)	350	6	1.2
B2	B11	35	4ϕ10 (0.47%)	350	6	1.2
B3	B12	45	4ϕ10 (0.47%)	350	6	1.2
B4	B13	25	4ϕ12 (0.67%)	350	6	1.2
B5	B14	25	4ϕ16 (1.2%)	350	6	1.2
B6	B15	25	4ϕ10 (0.47%)	450	6	1.2
B7	B16	25	4ϕ10 (0.47%)	550	6	1.2
B8	B17	25	4ϕ10 (0.47%)	350	8	1.8
B9	B18	25	4ϕ10 (0.47%)	350	10	2.6

A. Results

This section presents the results of all the beams analyzed in the parametric study. The results are presented in terms of the percentage of MR achieved for each beam and the load-maximum deflection relation at the sagging zones. Table 5 shows the results for beams B1’ to B9, while table 6 shows the results for beams B10 to B18. $M_{sag(FE)}$ and $M_{hog(FE)}$ are the sagging and hogging moment evaluated from the FE models. $M_{sag.el}$ and $M_{hog.el}$ and the percentages of change, M_{sag} & M_{hog} were calculated using equations 1,2,3 and 4 mentioned earlier. The percentages of MR enhancement were calculated relative to beam B1’ for beams B2 to B8, while the same percentages were calculated relative to beam B10 for beams B11 to B18.

B. Beams strengthened with steel plates

It was noticed from table 5 that the percentage of MR is increased with the increase in f_{cu} as was concluded from the results of beams B1’, B2 and B3. This is because the beams strengthened with 2 steel plates in the experimental program had failed as a result of the crushing the bottom concrete surface at the section near the intermediate support, and increasing the compressive strength will strengthen the compression side at the intermediate support section and will prevent or postpone the brittle crushing of the beams. Thus, allowing for more MR to take place. It was also observed that the increase in the steel bars reinforcement ratio negatively affects the MR, as noticed from the results of beams B1, B4 and B5. This could be due to the fact that increasing the cross-sectional area of the reinforcement steel bars would further enhance the strength of the tension side at the critical sections, leading to the increase of the opposing compression forces acting on the section to cause equilibrium. Consequently, this will result in early crushing of the concrete before MR is achieved to the maximum possible limit. It was also found out that MR decreases with the increase in beam thickness. However, MR is enhanced with the increase in the thickness of the applied plate due to the increase in the flexural stiffness of the strengthened section which causes the increase in the hogging moment at the intermediate support the expense of the sagging moments between supports. Figure 6 shows the relations between the applied loads and the maximum deflections measured at the sagging zones for all beams strengthened with steel plates.

C. Beam strengthened with CFRP plates

As we can see in table 6 that the percentage of MR was enhanced with the increase in the compressive strength of the concrete, which is the case in beams strengthened with steel plates. Moreover, increasing the reinforcement ratio has improved the values of MR recorded, opposing to the case of steel strengthening. This is because that the beams strengthened with CFRP plates in the experimental program has failed due to yielding of steel at one of the sections near the load application points, and increasing the reinforcement bars will strengthen the tension side at the sagging zones and will allow for more MR to be achieved. However, the percentages of MR were negatively affected with the increase in the beam thickness. Regarding the thickness of the CFRP laminates, it was found out that increasing the thickness of the laminate from 1.2 mm to 1.8 mm has enhanced MR by about 32% achieving an average percentage of 30%. However, the enhancement in MR was not as significant when the thickness of the plate was increased to 2.6 mm as the MR measured reached about 27%, which is less than that recorded when using the thinner laminate with 1.8 thickness. This is due to the debonding of the CFRP laminates from the concrete in beam B18, which indicates that increasing the thickness of the CFRP strengthening is not always in favor of MR enhancement. Figure 7 shows the relations between the applied loads and the maximum deflections measured at the sagging zones for all beams strengthened with steel plates.

Table 5. Results of the beams strengthened with steel plates

Specimen	P_u	$M_{sag(FE)}$	$M_{hog(FE)}$	$M_{sag.el}$	$M_{hog.el}$	[%] of change, M_{sag}	[%] of change, M_{hog}	Average [%] of MR	% of MR enhancement
	kN	kN.m							
B1’	601.	60.93	-179.07	94.0	-112.85	-35.21	58.68	46.95	
B2	718.	71.18	-216.82	112.	-134.69	-36.59	60.98	48.78	3.91
B3	776.	73.24	-241.77	121.	-145.59	-39.64	66.06	52.85	12.58
B4	663.	72.40	-186.80	103.	-124.35	-30.13	50.22	40.18	-14.42
B5	650.	78.31	-168.38	101.	-121.88	-22.89	38.16	30.52	-34.98
B6	768.	88.87	-206.33	120.	-144.03	-25.96	43.26	34.61	-26.28
B7	855.	109.3	-209.27	133.	-160.47	-18.24	30.41	24.33	-48.18
B8	611.	59.58	-186.43	95.4	-114.59	-37.61	62.69	50.15	6.83
B9	656.	62.81	-202.39	102.	-123.00	-38.72	64.54	51.63	9.98

(a) Typical failure mode (tension damage) in beams B1, SN1, SE1, CN1 & CN2

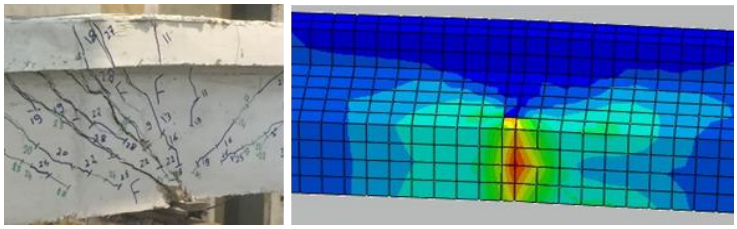

(b) Concrete crushing (compression damage) in beams SN2 & SE2

(c) Debonding of the CFRP plate in beam CE1

Fig. 5.FEM versus experimental failure modes

Table 6. Results of the beams strengthened with CFRP plates

Specimen	P_u	$M_{sag(FE)}$	$M_{hog(FE)}$	$M_{sag.el}$	$M_{hog.el}$	[%] of change, M_{sag}	[%] of change, M_{hog}	Average [%] of MR	% of MR enhancement
	kN	kN.m							
B10	491.04	63.72	-118.08	76.73	-92.07	-16.95	28.25	22.60	
B11	534.85	66.98	-133.47	83.57	-100.28	-19.86	33.09	26.47	17.14
B12	552.84	68.76	-138.90	86.38	-103.66	-20.40	34.00	27.20	20.35
B13	521	67.30	-125.90	81.41	-97.69	-17.33	28.88	23.10	2.23
B14	593.58	73.59	-149.61	92.75	-111.30	-20.66	34.43	27.54	21.86
B15	630.85	84.43	-146.58	98.57	-118.28	-14.35	23.92	19.13	-15.34
B16	794	108.40	-180.20	124.06	-148.88	-12.62	21.04	16.83	-25.52
B17	513.16	62.18	-132.22	80.18	-96.22	-22.45	37.42	29.93	32.45
B18	508.48	63.44	-127.36	79.45	-95.34	-20.15	33.59	26.87	18.88

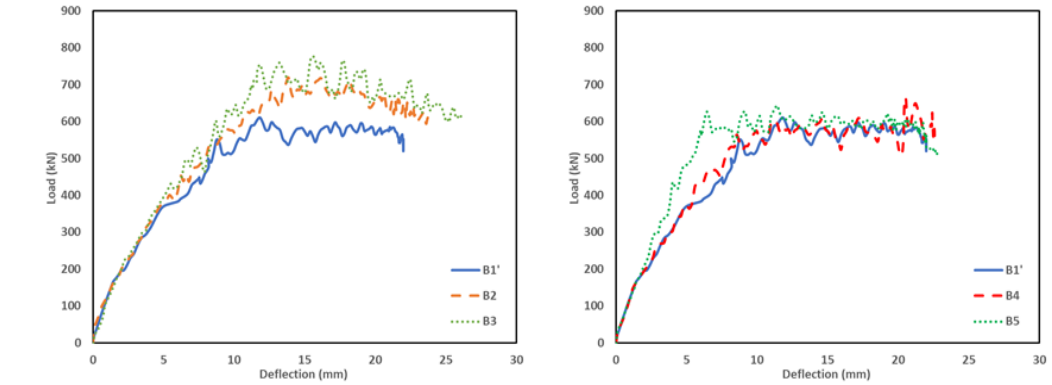

a) Load-midspan deflection for beams B1, B2 & B3 b) Load-midspan deflection for beams B1, B4 & B5

c) Load-midspan deflection for beams B1, B6 & B7 d) Load-midspan deflection for beams B1, B8 & B9

Fig. 6.Load-mid span deflection for beams strengthened with steel plates

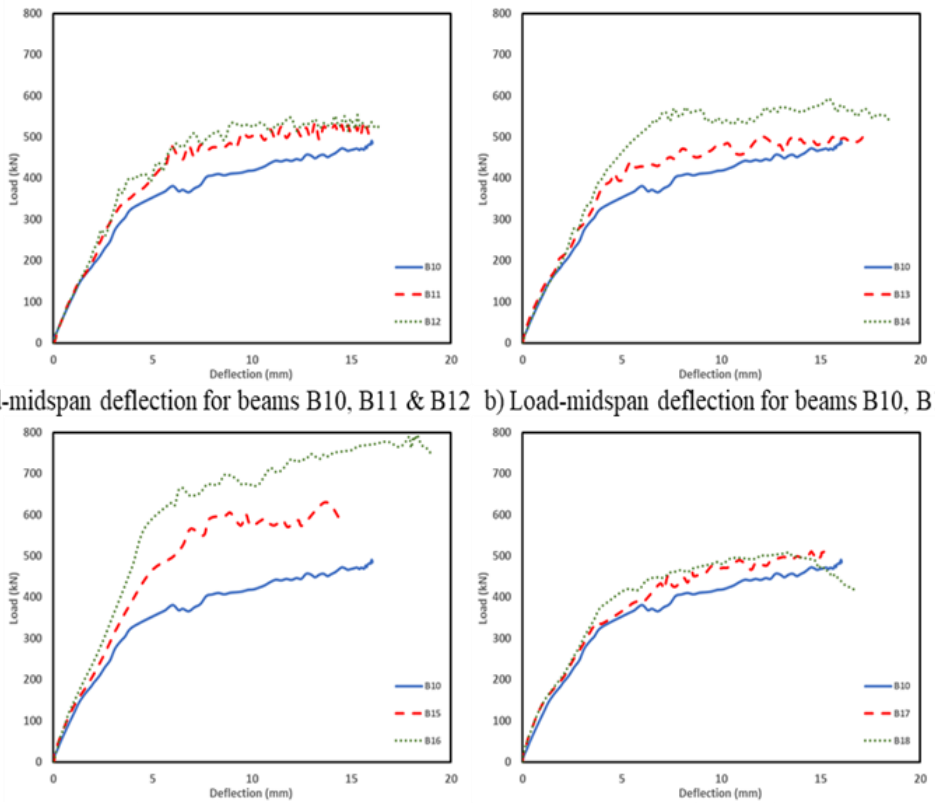

a) Load-midspan deflection for beams B10, B11 & B12 b) Load-midspan deflection for beams B10, B13 & B14

c) Load-midspan deflection for beams B10, B15 & B16 d) Load-midspan deflection for beams B10, B17 & B18

Fig. 7.Load-mid span deflection for beams strengthened with CFRP plates

VII. CONCLUSIONS

The NSM steel and CFRP plating technique at the hogging zones can cause up to 52 % and 30 % redistribution of moments from the sagging to the hogging regions respectively. It was also found that increasing the compressive strength of concrete enhances MR in continuous RC beams, while increasing the beam thickness reduces MR using either steel or CFRP top strengthening technique. Additionally, MR is enhanced with the increase in steel bars flexural reinforcement ratio in the beams top strengthened with 2 NSM CFRP laminates, while it is negatively affected by the increase in flexural reinforcement ratio in the beams top strengthened with steel plates. Moreover, higher thicknesses of the applied strengthening steel plates enhance MR in continuous RC beams. Furthermore, increasing the thickness of the strengthening NSM CFRP laminates enhances MR. However, debonding between CFRP and concrete tend to occur when using large thickness laminates.

REFERENCES

1. Hollaway LC and Leeming MB (1999) "Strengthening of Reinforced Concrete Structures". Woodhead Publishing, Cambridge, UK.
2. Teng JG, Chen JF, Smith ST and Lam L (2001) "FRP: Strengthened RC Structures". Wiley, New York, NY, USA.
3. Casadei P, Nanni A, Galati N, Ibell T and Denton S (2003) "Moment redistribution in continuous CFRP strengthened concrete members: experimental results". Proceedings of International Conference Composites in Construction – CCC2003, Cosenza, Italy, pp. 307–312.
4. El-Refaie SA, Ashour AF and Garrity SW (2003) "Sagging and hogging strengthening of continuous reinforced concrete beams using carbon fibre-reinforced polymer sheets". ACI Structural Journal 100(4): 446–453.
5. Oehlers D and Seracino R (2004) "Design of FRP and Steel Plated RC Structures: Retrofitting Beams and Slabs for Strength, Stiffness and Ductility". Elsevier, Amsterdam, The Netherlands.
6. Oehlers DJ, Ju G, Liu IST and Seracino R (2007) "A generic design approach for EB and NSM longitudinally plated RC beams". Construction and Building Materials 21(4): 697–708.
7. Kara I.F. and Ashour A.F., "Moment redistribution in Continuous FRP reinforced concrete beams," Construction and Building materials, vol. 49. pp. 939-948, December 2013.
8. Chen, J. F., and Teng, J. G. (2001). "Anchorage strength models for FRP and steel plates bonded to concrete." J. Struct. Eng., 127(7), 784–791.
9. De Lorenzis, L., and Nanni, A. (2002). "Bond between near-surface mounted fiber-reinforced polymer rods and concrete in structural strengthening." ACI Struct. J., 99(2), 123–132.
10. Yuan, H., Wu, Z. S., and Yoshizawa, H. (2001). "Theoretical solutions on interfacial stress transfer of externally bonded steel/composite laminates." J. Struct. Mech. Earthquake Eng., JSCE, 675(1-55), 27–39.
11. Mukhopadhyaya, P., Swamy, N., and Lynsdale, C. (1998). "Optimizing structural response of beams strengthened with GFRP plates." Journal of Composites for Construction, 2(2), 87–95.
12. ACI 318, Building code requirements for reinforced concrete and commentary, ACI 318-14, American Concrete Institute, Detroit, MI, 2014.
13. CSA/A23.3, Canadian Standard Association, Code for the design of concrete structures for buildings, CSA/A23.3-14, Toronto, Ontario, Canada, 2014.
14. Oehlers D.J., Ju G., Liu I.S.T. and Seracino R. (2004) "Moment redistribution in continuous plated RC flexural members. Part 1: neutral axis depth approach and tests," Engineering Structures, Vol 26, pp. 2197-2207.
15. Liu, I. S. T., Oehlers, D. J., and Seracino, R. (2006). "Tests on ductility of reinforced concrete beams retrofitted with FRP and steel near-surface mounted plates." Journal of Composites for Construction, 10(2), 106–114.
16. Ashour, A. F., El-Refaie, S. A., and Garrity, S. W. (2004). "Flexural strengthening of RC continuous beams using CFRP laminates." Cement and Concrete Composites, 26, 765–775.
17. Aiello M. A., Valente L. and Rizzo A. (2007). "Moment Redistribution in Continuous Reinforced Concrete Beams Strengthened with Carbon Fiber-Reinforced Polymer Laminates." Mechanics of Composite Materials, Vol. 43, No. 5, pp. 667-686.
18. ABAQUS, Theory Manual Version 6.14, Dassault Systems, 2014.

AUTHORS PROFILE

Amr Ibrahim is a PhD candidate who is currently working as a lecturer assistant in the civil engineering department at the British University in Egypt, He earned his BSc. Degree from Ain Shams University in 2009. He received his MSc. Degree from the same University in 2015. His research interests include design of reinforced concrete structures, composite materials and the application of Fiber Reinforced Plastics in concrete structures.

Prof. Khalil is a professor of reinforced concrete structures at Ain Shams University, he earned his PhD degree from Iowa State University in 1998. He has over twenty-five years of Experience in Structural Engineering fields. He has been teaching for both undergraduate and graduate levels. His research interests include design of reinforced concrete structures, Pre-stressed concrete and Bridge Engineering

Dr. Salem is a member of the ASCE Risk and Resilience Measurements committee, and the Social Science, Policy, Economics and Education Decision committee. He is also a member SEI blast protection of buildings standards committee. Dr. Salem has received Engineering Mechanics Institute Objective resilience award. He served as a reviewer for the Journal of Structural Engineering (ASCE) and the Construction and Buildings Materials Journal.

Dr. El-kateb received his BSc. degree from Ain Shams University in 1999, He earned his MSc. And PhD degrees from the same University in 2007 and 2013. He is working as a full-time assistant professor in the structural engineering department at Ain Shams University. His career as a structural engineer has extended for over 20 years of professional experience and academic practice, with many publications in peer-reviewed international journals.